PROCEEDINGS B

royalsocietypublishing.org/journal/rspb

Research

Cite this article: Rolshausen G, Hallman U, Grande FD, Otte J, Knudsen K, Schmitt I. 2020 Expanding the mutualistic niche: parallel symbiont turnover along climatic gradients. *Proc. R. Soc. B* **287**: 20192311.
http://dx.doi.org/10.1098/rspb.2019.2311

Received: 2 October 2019
Accepted: 6 March 2020

Subject Category:
Ecology

Subject Areas:
ecology, microbiology, evolution

Keywords:
mutualist-mediated effects, facilitation, range predictions, beta-diversity turnover, altitude-for-latitude, lichen symbiosis

Author for correspondence:
Gregor Rolshausen
email: grolshausen@senckenberg.de

Electronic supplementary material is available online at https://doi.org/10.6084/m9.figshare.c.4893387.

THE ROYAL SOCIETY PUBLISHING

Expanding the mutualistic niche: parallel symbiont turnover along climatic gradients

Gregor Rolshausen[1], Uwe Hallman[1], Francesco Dal Grande[1], Jürgen Otte[1], Kerry Knudsen[2] and Imke Schmitt[1,3]

[1]Senckenberg Biodiversity and Climate Research Centre (SBiK-F), Frankfurt am Main, Germany
[2]Department of Ecology, Czech University of Life Sciences Prague | CULS, Prague, Czech Republic
[3]Departement of Biological Sciences, Goethe University, Frankfurt am Main, Germany

GR, 0000-0003-1398-7396

Keystone mutualisms, such as corals, lichens or mycorrhizae, sustain fundamental ecosystem functions. Range dynamics of these symbioses are, however, inherently difficult to predict because host species may switch between different symbiont partners in different environments, thereby altering the range of the mutualism as a functional unit. Biogeographic models of mutualisms thus have to consider both the ecological amplitudes of various symbiont partners and the abiotic conditions that trigger symbiont replacement. To address this challenge, we here investigate 'symbiont turnover zones'—defined as demarcated regions where symbiont replacement is most likely to occur, as indicated by overlapping abundances of symbiont ecotypes. Mapping the distribution of algal symbionts from two species of lichen-forming fungi along four independent altitudinal gradients, we detected an abrupt and consistent β-diversity turnover suggesting parallel niche partitioning. Modelling contrasting environmental response functions obtained from latitudinal distributions of algal ecotypes consistently predicted a confined altitudinal turnover zone. In all gradients this symbiont turnover zone is characterized by approximately 12°C average annual temperature and approximately 5°C mean temperature of the coldest quarter, marking the transition from Mediterranean to cool temperate bioregions. Integrating the conditions of symbiont turnover into biogeographic models of mutualisms is an important step towards a comprehensive understanding of biodiversity dynamics under ongoing environmental change.

1. Introduction

The distributional range of a mutualistic symbiosis is largely determined by the ecological amplitudes of its interacting species. Scarcity of suitable interaction partners can restrict the potential niche of a symbiosis [1–3], whereas the acquisition and replacement of symbionts adapted to different environmental conditions can broaden the niche of a host taxon [4–8]. Such mutualist-mediated niche dynamics are particularly evident along environmental gradients where the distribution of genetic diversity in host–symbiont combinations can closely correspond to transitions between distinct abiotic conditions. Prominent examples of these spatially structured interactions between a host and its symbionts include the light-dependent zonation of dinoflagellate symbionts associated with coral hosts along marine depth gradients [9–12], the replacement of mycorrhizal fungi along soil nitrogen gradients [13–15] and the turnover of genetic lineages of green algal symbionts associated with lichen-forming fungi along altitudinal and latitudinal gradients [16–18]. Notably, such spatial genetic structuring in mutualist-mediated niches also implies the presence of demarcated transition zones where symbiont replacement is most likely to occur (figure 1). These 'symbiont turnover zones' are an integral, but hitherto unspecified, part of the mutualistic niche concept [5,19,20], where they depict the distributional boundaries

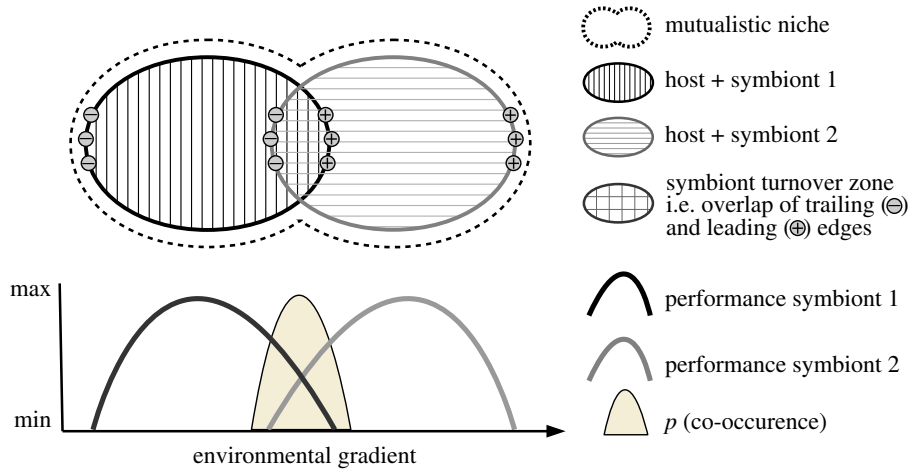

Figure 1. The mutualistic niche space of a symbiotic host can be subdivided into separate sections, each of which depends on the presence of particular symbionts (1 and 2) with distinct performance optima along the respective niche axes (i.e. the mutualistic niche). The location where a switch from one symbiont to another is expected to take place is where trailing or leading edges of different symbiont populations overlap (i.e. the symbiont turnover zone). (Online version in colour.)

(i.e. the trailing and leading edges) of particular host–symbiont combinations within the full range of a mutualism.

Since trailing and leading edges of populations are particularly sensitive to shifting environmental selection [21–26], symbiont turnover zones are likely to be critically important to understand a mutualism's response to climate change. For instance, a given shift in climatic selection can differentially affect mutualists with different physiological optima, thereby decoupling the rates at which their trailing and leading edge populations track their climatic niche [27–29]. As a consequence, symbiont turnover zones might experience contraction, expansion or disruption under ongoing shifts in selection. Similarly, the ability of a host species to alter its range in response to climate change will depend on the available physiological variation among its symbionts [5,19,30,31]. Hence, considering symbiont diversity together with the environmental conditions that underlie symbiont turnover will improve predictions of how abundances and ranges of keystone mutualisms will shift in the future. Likewise, correctly locating turnover zones will allow us to pinpoint geographic areas particularly sensitive to disturbance, because these zones are expected to experience stark changes in taxonomic diversity and composition under climate change and other anthropogenic stressors.

Lichens constitute obligate mutualisms in which a fungal partner (mycobiont) hosts photosynthetic algae and/or cyanobacteria (photobionts) in a characteristic thallus structure. Due to their low dispersal limitations and their ability to withstand frequent cycles of drying and wetting, some lichen species occur across large distributional areas and steep ecological gradients [32–34]. Moreover, some mycobionts associate with different photobiont lineages throughout their distributional range [35–38], presumably to maintain high photosynthetic carbon gains beyond the range margins of a single photobiont strain. Spatial structuring of photobionts associated with a lichen host has been documented along latitudinal [18,39] as well as altitudinal gradients [17], suggesting symbiont turnover as a result of shifting environmental selection. However, it is unclear whether symbiont turnover in lichens is gradual or abrupt, and whether explicit turnover zones can be identified or geographically located. Consequently, we also lack an understanding of the particular environmental conditions associated with photobiont replacement. Moreover, testing whether there are universal conditions for photobiont replacement ultimately requires repeated predictability of turnover patterns from similar environmental variables (i.e. parallelism [40–42]) along independent gradients and in multiple species of hosts and symbionts.

To address the above knowledge gaps, we here define the symbiont turnover zone of a mutualistic symbiosis as the area of the highest co-occurrence probability of symbionts with distinct performance optima. For instance, along an altitudinal gradient, a local turnover zone will envelope both the leading edge of symbionts adapted to low-altitude conditions and the trailing edge of symbionts adapted to high-altitude conditions (figure 1). Moreover, due to selective differentiation towards the edges of the turnover zone, genetic community composition on either side of the zone should show minimal overlap. Hence, the patterns of symbiont β-diversity across the zone are expected to be primarily caused by spatial taxonomic turnover rather than by nested subsets of taxa. We apply this framework using population-level sampling of two lichen host species and their phylogenetically distinct green algal symbionts along replicated altitudinal gradients in western North America and Europe.

To examine general predictability of turnover patterns, we then use algal ecotype response functions that were modelled along a broad-scale latitudinal gradient in Europe to project turnover predictions onto the aforementioned altitudinal gradients. Specifically, we ask the following questions. (i) Is there parallel spatial structuring of photobionts in lichens along replicated environmental gradients? (ii) Which climatic conditions are associated with photobiont replacements in lichens? (iii) Can we predict a universal altitudinal turnover zone from model-based occurrence probabilities of distinct symbiont ecotypes using information from latitudinal distributions?

2. Material and methods

(a) Photobiont sampling and genotyping

Field sampling of lichen thalli was carried out along four altitudinal gradients: Mount Limbara (Sardinia, Italy; 8 sites); Sierra de Gredos (Sistema Central, Spain; 6 sites); Mount San Jacinto (California, USA; 7 sites); and Sierra Nevada (California, USA; 4 sites). Both lichen species in our study, *Umbilicaria pustulata*

(reduced to synonymy with *Lasallia pustulata)* in Europe and *Umbilicaria phaea* in North America, hosted green algae of the genus *Trebouxia* as photobionts. Detailed information about sampling locations and sampling extent is given in electronic supplementary material, table S1. At each sampling site, small parts of lichen thalli were collected over an area of roughly 100 m² with a minimum distance of 0.5 m between individual thalli, aiming to capture the maximal diversity at each site. From all samples, total genomic DNA was extracted using a small part of the thallus following the CTAB protocol [43]. Algal symbionts were sequenced at the internal transcribed spacer region nrITS rDNA using primers nrITS1T (f) and nrITS4T (r) based on [44]. PCR amplification, amplicon sequencing and sequence alignment followed established protocols for umbilicate lichens described in [45,46]. *Trebouxia* sequence identities were confirmed using BLAST searches in GenBank. Algal diversity at each sampling site was then analysed at the level of the dominant ITS haplotype (i.e. greater than 70% of total abundance) in each thallus sample [47]. Detailed information about *Trebouxia* ITS haplotypes recovered in this study is given in electronic supplementary material, table S2, together with GenBank accession numbers. A phylogenetic tree comparing ITS sequences of our study to the 69 ITS OTUs underlying a widely used classification system for *Trebouxia* photobionts [48] was calculated using RaxML [49] and is shown in electronic supplementary material, figure S1.

(b) Climatic profiles along environmental gradients

Models of ecotype response functions (introduced below) were restricted to a non-exhaustive set of 10 bioclimatic variables (electronic supplementary material, table S3) that could be reliably obtained for each of the four altitudinal gradients. For the two European gradients (Mount Limbara and Sierra de Gredos), bioclimatic variables were drawn from the WorldClim database [50] at the highest spatial resolution (approx. 1 km). For the two North American gradients (Mount San Jacinto and Sierra Nevada), we used data resources from the PRISM climate group (PRISM Climate Group, Oregon State University, www.prism.oregonstate.edu). Along each gradient, we chose 20 ascending climatic sample locations and extracted temperature variables (monthly min, max and average °C), and precipitation estimates (mm) to calculate the respective bioclimatic variables. For all four gradients, we then used generalized additive models (GAMs) regressing climate variables against altitude to predict a new set of 200 bioclim datapoints along each gradient spanning from 100 m to 2700 m altitude. This new set of gradient-specific model-based climate variables was then used to project ecotype response function models onto each gradient. We note that the used data sources (WorldClim and PRISM) do not consider effects of slope or aspect on mountain climate; as a result, the fine-scale accuracy of model projections may differ between individual gradients. Climatic variables for the latitudinal gradient across Europe were obtained from WorldClim [50] based on sampling described in [18].

(c) Modelling and predicting environmental response functions

To achieve sufficient climatic resolution and predictive power in ecotype response functions, we trained logistic GAMs based on a large-scale latitudinal dataset of two distinct *Trebouxia* ecotype clusters from warm and cool temperate biomes across Europe: the arctic–alpine ecotype and the Mediterranean ecotype described in [18]. In particular, these ecotypes were chosen because their contrasting climatic preferences encompass the observed climatic range experienced across the altitudinal turnover zones. The occurrence probability distributions along each bioclimatic variable obtained this way were then used to calculate the co-occurence probability as the product of the respective response functions (electronic supplementary material, figure S2). Using the 200 model-based bioclimatic datapoints along each of the four altitudinal gradients (see above), we then projected co-occurence probabilities of the warm- and cold-preferring algal ecotypes (i.e. symbiont turnover probabilities; electronic supplementary material, figure S2) onto each gradient. We applied this framework to each of the 10 bioclimatic variables separately, as well as to three more complex GAMs that included two predictors and their tensor product interaction terms, respectively. For the latter framework, we chose three pairs of predictor variables to address critical moisture availability during the driest quarter (BIO9 ⊗ BIO17), the warmest quarter (BIO10 ⊗ BIO18) and the coldest quarter (BIO11 ⊗ BIO19). All trained GAMs were evaluated based on combined AIC scores (electronic supplementary material, figure S3) to obtain the best predictive models for single predictor variables and variable interactions. Results from the model predictions for each gradient (i.e. co-occurence probabilities of both ecotypes) were plotted along altitude together with their 95%CIs obtained from the GAM output. All GAM models used restricted maximum likelihood (REML) to estimate smoothing parameters and were implemented using the *mgcv* package in R [51–53].

(d) diversity, turnover and diversity ordinations

β-diversity among sampling sites was calculated based on Jaccard dissimilarity, using the R package *vegan* [54]. Distance matrices were then further partitioned into turnover versus nestedness components using the R package *betapart* [55], of which we report the turnover component. Congruence between predicted turnover (derived from co-occurence probabilities) and observed turnover (derived from Jaccard dissimilarities) along gradients was evaluated by Procrustean superimposition of pairwise turnover distances between sampling sites and their relative distances to the peak of the prediction curve (see electronic supplementary material for details). To investigate regional diversity within the two (continental) pools of *Trebouxia* photobionts independent from a particular gradient, we combined data from both European gradients and from both North American gradients, respectively. For each pool, we calculated Jaccard dissimilarity matrices depicting the diversity between sampling sites. These matrices were then visualized using NMDS ordinations that were rotated to altitude to better depict the relationship between low-altitude and high-altitude diversity.

3. Results

(a) Symbiont diversity along altitudinal gradients

Analyses of population genetic diversity at the algal ITS locus revealed that the *Trebouxia* communities in *U. pustulata* from Europe were highly differentiated from those in *U. phaea* from North America (electronic supplementary material, figure S1). Overall, our study reveals widespread geographic distributions of identical algal lineages (greater than 800 km, across each continent) coupled with concentrated local structuring (less than 10 km, along each gradient), indicating that photobiont distributions are governed by climate rather than by dispersal limitations at the continental scale. Within both photobiont community pools, we found marked spatial genetic structure indicating altitudinal niche partitioning along replicated gradients that coincided with the transition from the warm temperate (Mediterranean) to the cool temperate biome (figure 2*a*,*b*). Moreover, partitioning of Jaccard dissimilarity and focusing on the turnover component among sampling sites (i.e. non-nestedness [56–58]) confirmed

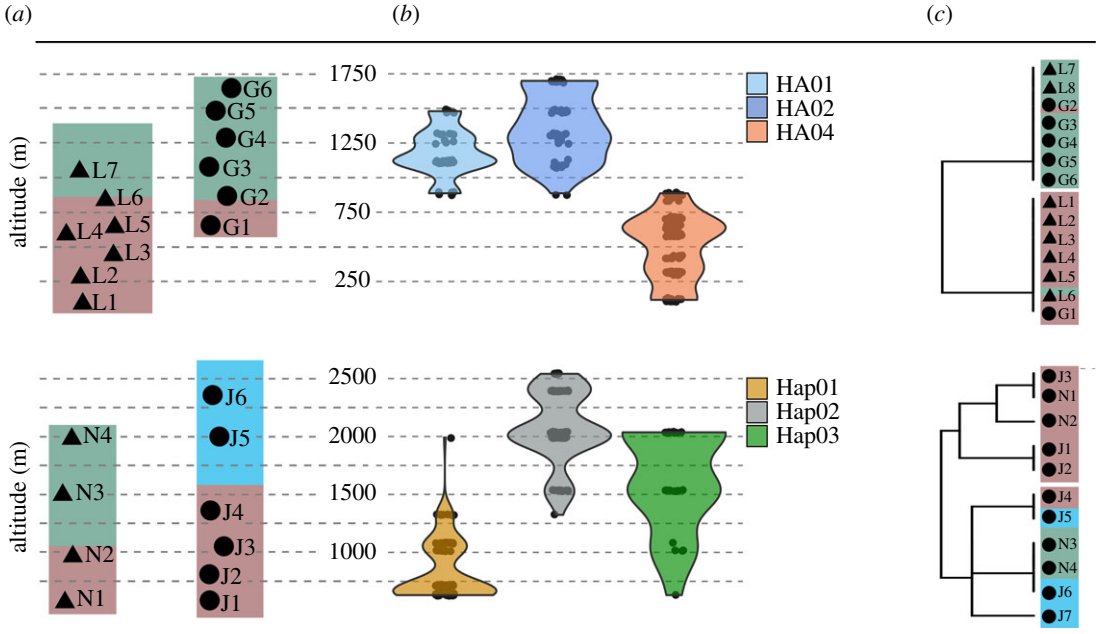

Figure 2. Spatial niche partitioning among *Trebouxia* symbionts along four independent altitudinal gradients. Upper panel depicts sampling sites in Europe (L1–7: Mount Limbara; G1–6: Sierra de Gredos); lower panel depicts sampling sites in California (N1–4: Sierra Nevada; J1–7: Mount San Jacinto). (*a*) Sampling sites along each gradient with colours indicating climate strata (I–III) derived from cluster analysis of 10 bioclimatic variables (electronic supplementary material, table S3). Shared *y*-axis depicts altitude in metres. (*b*) Violin plots of abundance distributions for the three most common algal haplotypes, based on pooled sampling sites within Europe and North America respectively. (*c*) Turnover among algal symbionts, calculated across sampling sites. The turnover component (i.e. β-diversity) is based on partitioned Jaccard dissimilarity matrices and is visualized with dendrograms. Background colours of tips refer to the same climate strata as indicated in (*a*). (Online version in colour.)

taxonomic replacement—rather than nestedness—as the predominant structural pattern of photobiont β-diversity between high-altitude and low-altitude sites (figure 2*c*). This pattern was also confirmed with diversity NMDS ordinations clearly separating sites by altitude independent of a particular gradient (electronic supplementary material, figure S4). Together, these results suggest that similar ecological segregation among geographically independent and phylogenetically distinct photobiont communities (i.e. ecotypes) promotes parallel climatic niche expansions from low to high altitudes in both species of lichenized fungi. Consequently, our sampling sites along each of the four mountain slopes should encompass similar symbiont turnover zones where contrasting photobiont ecotypes co-occur at their trailing and leading edges, respectively (figure 1). We used GAM of *Trebouxia* ecotype response functions to predict the exact locations of these zones and to test which climatic variables underlie the observed parallelism in niche expansions of the lichen symbiosis.

(b) Predicting symbiont turnover zones

Latitudinal GAMs were first evaluated based on AIC comparison (electronic supplementary material, figure S3), and niche predictions from the best-performing GAMs (i.e. combined $\Delta AIC < 10$) were then projected onto the four altitudinal gradients to find the areas of maximized ecotype co-occurrence (i.e. symbiont turnover zones; electronic supplementary material, figure S2). Applying this GAM framework to ten climatic variables (electronic supplementary material, table S3) revealed that mean annual temperature (BIO1) together with mean temperature of the coldest quarter (BIO11) were the strongest univariate predictors that accurately located symbiont turnover zones along each gradient. Specifically, GAM predictions based on variables BIO1 and BIO11 correctly placed local maxima of ecotype co-occurrence at altitudes congruent with the actual photobiont β-diversity turnover recorded along each gradient (figure 3*a*; electronic supplementary material, figure S5). Correspondingly, symbiont communities on either side of the predicted local co-occurence maxima were more similar to each other than expected from random association (European gradients: $r_{BIO1} = 0.80$, $p < 0.005$; $r_{BIO11} = 0.70$, $p < 0.01$; Californian gradients: $r_{BIO1} = 0.82$, $p < 0.01$; $r_{BIO11} = 0.72$, $p < 0.01$; Procrustes superimposition of distance matrices). The turnover zones depicted in this way were similar in width and were characterized by similar temperature regimes (table 1). Peak levels of ecotype co-occurrence were predicted to occur across a delimited altitudinal belt, approximately 150–200 m wide, and located at different altitudes at each gradient (figure 3*a*; electronic supplementary material, figure S5). None of the single precipitation variables included in our analyses successfully predicted local maxima of co-occurrence that were congruent with the observed photobiont turnover (electronic supplementary material, figure S5). Yet, modelling the interaction of precipitation and temperature again confirmed turnover zones centred in between high- and low-altitude communities from Europe and North America, respectively. More specifically, GAM predictions from interactions between precipitation and temperature of the warmest quarter (BIO10 ⊗ BIO18) performed best across all gradients (electronic supplementary material, figure S3 for ΔAICs) and correctly located ecotype co-occurrence maxima near the centre of community distance-based β-diversity turnover (European gradients: $r_{BIO10 \otimes BIO18} = 0.61$, $p < 0.05$;

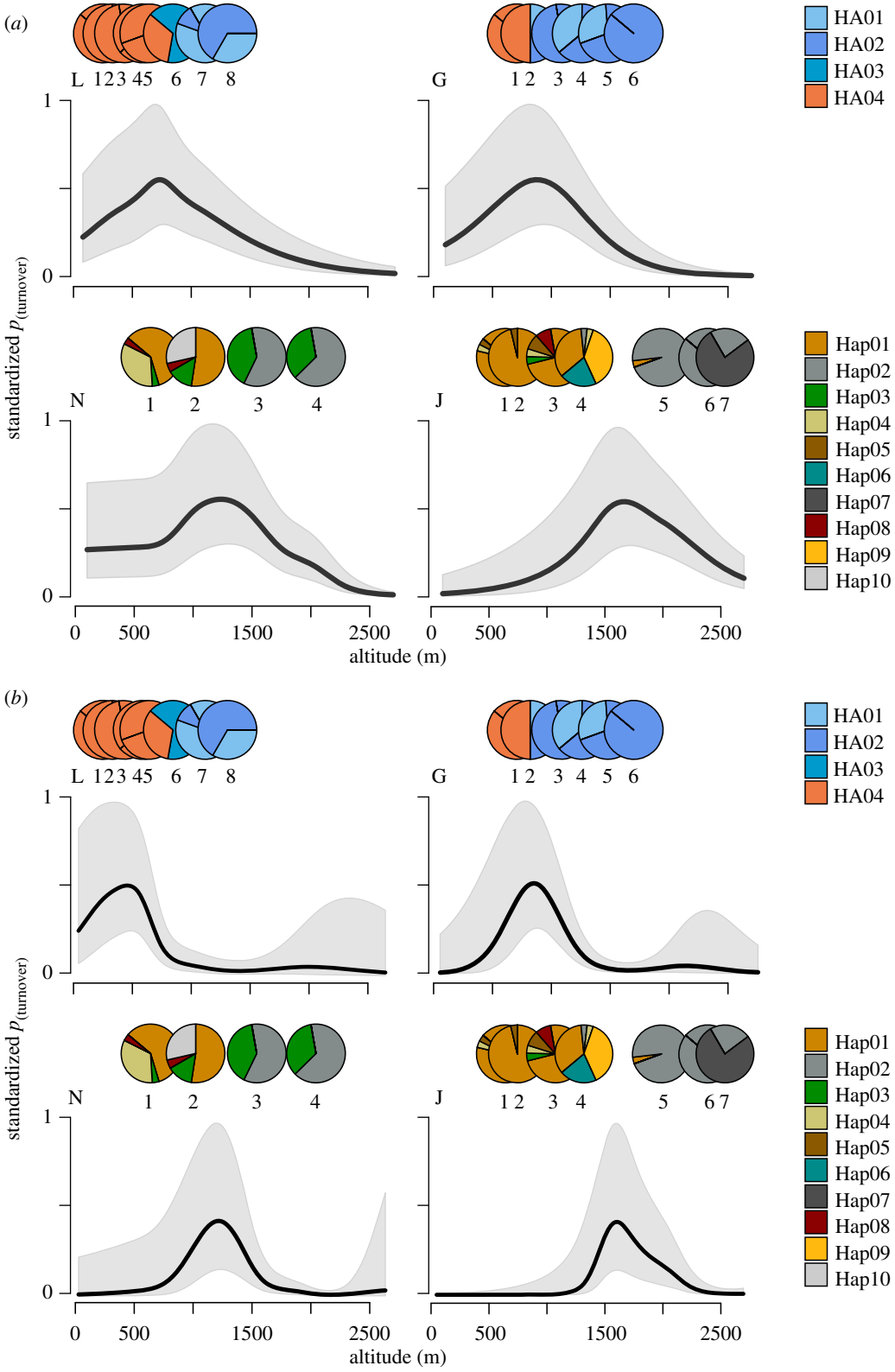

Figure 3. Prediction of symbiont turnover zones. (*a*,*b*) Model-based prediction of co-occurrence probability for warm and cold temperate algal ecotypes standardized to a maximum of 1 (black line +95%CI in grey) along each particular gradient. Predictions are based on (*a*) single variable GAMs for mean annual temperature (BIO1) and (*b*) on the interaction of temperature and precipitation during the warmest quarter (BIO10 ⊗ BIO18). Peaks indicate highest probability of co-occurrence; i.e. the centre of a turnover zone. Letters indicate the gradients (L: Mount Limbara; G: Sierra de Gredos; N: Sierra Nevada; J: Mount San Jacinto). Pie charts above each plot depict the on-site sampled abundance distributions of algal haplotypes with numbers depicting sampling sites (electronic supplementary material, table S1). (Online version in colour.)

Californian gradients: $r_{BIO10 \otimes BIO18} = 0.69$, $p < 0.05$; figure 3*b*). The results for all tested interaction terms are depicted in electronic supplementary material, figure S6. In addition, the interaction between precipitation and temperature of the coldest quarter (BIO11 ⊗ BIO19) was an important predictor of turnover, yet only at one of the four gradients (Mount Limbara: $r_{BIO11 \otimes BIO19} = 0.81$, $p < 0.05$; electronic supplementary material, figure S6).

Table 1. Altitudinal location and temperature profiles for the predicted turnover zones along each of the four gradients. Values represent average temperatures (± s.d.) of a confined zone around the peak of the co-occurence probability curves. Variable selection was based on ΔAIC and prediction accuracy (i.e. comparing peak location to observed turnover location).

		average temperature (°C)	
gradient	altitude (m)	annual	coldest quarter
Mount Limbara	~700–800	12.31 ± 0.30	5.69 ± 0.27
Sierra de Gredos	~900–1000	12.04 ± 0.15	4.41 ± 0.13
Sierra Nevada	~1200–1300	12.30 ± 0.13	4.88 ± 0.10
Mount San Jacinto	~1600–1700	12.45 ± 0.20	5.31 ± 0.18

In summary, we show that photobiont turnover zones could be repeatedly predicted from the same set of niche parameters (i.e. temperature and temperature x precipitation) along independent altitudinal gradients. The GAM framework underlying these predictions was trained and evaluated on the occurrence data of photobiont ecotype clusters along a Europe-wide latitudinal climatic gradient. Our results thus indicate (i) parallel spatial structuring and niche partitioning of photobionts in lichens along replicated environmental gradients, (ii) annual average temperature, average temperature of the coldest quarter and critical moisture availability during the warmest quarter as the climatic drivers of photobiont replacement and (iii) similar climatic selection regimes underlying predictable symbiont replacements along latitudinal and altitudinal gradients.

4. Discussion

The mutualistic niche concept states that the realized niche space of a mutualistic host can be expanded by the availability and replacement of symbionts with distinct, non-overlapping performance optima along particular niche axes [5,19,20]. Our study highlights the significance of locally confined symbiont turnover zones as an integral and useful part of this concept. In particular, we show that studying turnover zones along environmental gradients provides a crucial first step to scrutinize the ecological processes underlying mutualist-mediated niche dynamics. We argue that symbiont turnover zones serve to address two key hypotheses in the mutualistic niche concept: (i) variation in performance optima among symbionts stabilizes the benefit for mutualists that associate with multiple partners across their realized niche space (portfolio effect [20,59]); and (ii) similar environmental transitions promote similar symbiont turnover patterns in independent niche expansions (parallelism).

Lichen-forming fungi are known to exhibit distinctly structured photobiont communities throughout their distributional ranges [16,17,37,60]. Recent niche modelling studies show that unique portions of a lichen's overall niche space can be partitioned among genetically distinct photobiont lineages [18,39], thus suggesting that particular environmental transitions probably evoke symbiont replacements. Our current investigation of symbiont turnover zones lends general support for this hypothesis. For the first time, we show that photobiont turnover (i.e. non-nested β-diversity) along independent altitudinal gradients in Spain, Italy and California takes place abruptly and across confined zones characterized by similar climatic conditions (figure 2). Accordingly, diversity ordinations based on pooled sampling sites in Europe and California, respectively, show significant separation of low-altitude versus high-altitude communities, independent of individual gradients (electronic supplementary material, figure S4). Such strong non-nested spatial segregation between genetically closely related types with low dispersal limitation indicates climatic niche partitioning of photobionts along the altitudinal gradient. Moreover, we find that the approximate location of symbiont turnover along each gradient is predictable from climatic response functions of distinct photobiont ecotypes from a latitudinal gradient across Europe. Notably, prediction accuracy was independent of lichen host species or phylogenetic background of the *Trebouxia* photobionts. The examination of turnover zones thus strongly suggests parallel range expansions from low- to high-altitude (and latitude) habitats based on convergent diversification of symbiont ecotypes. Likewise, given the broad host spectrum and extensive biogeographical range of *Trebouxia* photobionts [35,48,61–63], the pattern we describe conceivably applies to other lichen species as well.

We used AIC model selection together with prediction accuracy of different response functions as an indicator to ask which transitions in which climatic variables most likely evoke symbiont turnover. From the non-exhaustive list of climatic variables we tested, temperature was the most accurate predictor of altitudinal symbiont turnover. More specifically, turnover zones were characterized by a mean annual temperature (BIO1) of approximately 12°C and a mean temperature of the coldest quarter (BIO11) of approximately 5°C (table 1). In addition, critical moisture availability, depicted here by the interaction of temperature (BIO10) and precipitation (BIO18) during the warmest quarter, was found to be an important predictor of photobiont turnover across all gradients (figure 3*b*). Together, these values indicate that the studied turnover zones bridge the climatic transition from warm temperate to cool temperate biomes [64]. Similar climatic transitions have been shown to impact photosynthetic performance and to promote ecotype differentiation in other lichen species, both experimentally [65–70] and bio-geographically [16,17,71]. Nonetheless, explicitly applying the concept of turnover zones, we here show—for the first time—a general and predictable pattern of climate-driven symbiont replacement that corroborates previous hypotheses of symbiont-mediated niche expansions in lichens.

We note, however, that the single-marker approach we use will only depict the dominant photobiont lineage (i.e. greater than 70% of total abundance) for each sample [47], thereby ignoring the presence of multiple symbionts in a single thallus [17,69,72]. Hence, despite the clear turnover pattern in (dominant) photobionts, our data are indeed insufficient to distinguish between two mutually non-exclusive hypotheses for the cause of this pattern. On the one hand, lichen turnover zones might be primarily caused by environmental filters that target contrasting physiological adaptations in photobionts [70,71]. This scenario is in accordance with a dynamic niche expansion that is indeed contingent on the availability of distinct symbiont ecotypes providing

benefits to the host. On the other hand, turnover among dominant photobionts might also be caused by variation in intraspecific competition among algal lineages within the same lichen thallus, irrespective of benefits to the host. Given that competitive dominance depends on environmental conditions [73,74], the latter scenario would thus result in similar convergence among symbionts across the turnover zones; yet the niche dynamics of the host would not be genuinely symbiont mediated. Nonetheless, the consistency in the environmental transitions we find for independent symbiont turnover zones provides a valuable starting point for going forward in testing competing hypotheses. In particular, informed experiments are needed to investigate whether climatic conditions on either side of the turnover zone differentially affect photosynthesis and/or competitive ability in different algal strains [69–71].

In conclusion, the characterization of symbiont turnover zones is a promising step toward a better understanding of mutualist-mediated niche dynamics, particularly in obligate symbioses such as corals, lichens or mycorrhizae. To study the role of different symbiont partners in expanding a host's niche breadth, it makes sense to investigate the environmental transitions that promote compositional turnover among those symbionts. The insights thus gained allow for a better description of environmental selection pressures underlying mutualistic range expansions (or contractions). Moreover, it is vitally important to explicitly consider conditions of symbiont turnover in the predictions of range limits and/or climate change responses of mutualisms. We here suggest a two-step framework to locate and verify turnover zones along environmental gradients based on a detailed characterization of β-diversity (i.e. turnover versus nestedness) and model-based inference of symbiont co-occurence probability. As an example, we demonstrate symbiont turnover zones within the mutualistic niches of lichen-forming fungi and their algal symbionts along independent environmental gradients. We identify consistent transitions in temperature and critical moisture availability associated with parallel symbiont replacements, thereby informing future research regarding the extent of ecotypic differentiation among algal symbionts in lichens. In general, similar work addressing the resilience of symbiotic interactions toward ongoing environmental change will benefit from incorporating symbiont turnover zones into the concept of the mutualistic niche.

Data accessibility. The data supporting the results are uploaded to the Dryad Data Repository: https://doi.org/10.5061/dryad.qv9s4mw9s [75]. GenBank accession numbers are provided as part of the electronic supplementary material.

Authors' contributions. I.S. and K.K. conducted field work and sampling; U.H. curated the data; J.O. performed laboratory work; G.R. analysed the data and wrote the manuscript, with input from I.S. and F.D.G.

Competing interests. We declare we have no competing interests.

Funding. This work was financially supported by the research funding program Landes-Offensive zur Entwicklung Wissenschaftlich-Oekonomischer Exzellenz (LOEWE) of Hesse's Ministry of Higher Education, Research, and the Arts through the Senckenberg Biodiversity and Climate Research Centre (SBiK-F). K.K. was financially supported by the grant of Ministry of Education, Youth and Sports of the Czech Republic, program of international cooperation between the Czech Republic and USA for research, development and innovations, grant no. LTAUSA18188.

Acknowledgements. We gratefully acknowledge the following colleagues for support with field work and advice on sampling: Jana Kocourková (Univ. of Prague), Julia Adams (UC Riverside), John Taylor, Tom Bruns (both UC Berkeley), Mike Hamilton (Blue Oak Ranch Reserve), Bruce McCune (Oregon State Univ.), Ellen Dean, Jean Shepard (both UC Davis), Anna Sadowska-Deś (Univ. of Frankfurt) and Mercedes Vivas (Univ. Complutense, Madrid). Miklós Bálint, Thomas Hickler and Liam Langan (Senckenberg SBiK-F) gave helpful comments on an earlier version of the manuscript. Also, we thank the reviewers for valuable comments on the manuscript.

References

1. Weber A, Karst J, Gilbert B, Kimmins JP. 2005 *Thuja plicata* exclusion in ectomycorrhiza-dominated forests: testing the role of inoculum potential of arbuscular mycorrhizal fungi. *Oecologia* **143**, 148–156. (doi:10.1007/s00442-004-1777-y)
2. Nuñez MA, Horton TR, Simberloff D. 2009 Lack of belowground mutualisms hinders Pinaceae invasions. *Ecology* **90**, 2352–2359. (doi:10.1890/08-2139.1)
3. Mueller UG *et al.* 2011 Evolution of cold-tolerant fungal symbionts permits winter fungiculture by leafcutter ants at the northern frontier of a tropical ant–fungus symbiosis. *Proc. Natl Acad. Sci. USA* **108**, 4053–4056. (doi:10.1073/pnas.1015806108)
4. Marquez LM, Redman RS, Rodriguez RJ, Roossinck MJ. 2007 A virus in a fungus in a plant: three-way symbiosis required for thermal tolerance. *Science* **315**, 513–515. (doi:10.1126/science.1136237)
5. Afkhami ME, McIntyre PJ, Strauss SY. 2014 Mutualist-mediated effects on species' range limits across large geographic scales. *Ecol. Lett.* **17**, 1265–1273. (doi:10.1111/ele.12332)
6. Maher AMD, Asaiyah MAM, Brophy C, Griffin CT. 2017 An entomopathogenic nematode extends its niche by associating with different symbionts. *Microb. Ecol.* **73**, 211–223. (doi:10.1007/s00248-016-0829-2)
7. Sudakaran S, Kost C, Kaltenpoth M. 2017 Symbiont acquisition and replacement as a source of ecological innovation. *Trends Microbiol.* **25**, 375–390. (doi:10.1016/j.tim.2017.02.014)
8. Pither J, Pickles BJ, Simard SW, Ordonez A, Williams JW. 2018 Below-ground biotic interactions moderated the postglacial range dynamics of trees. *New Phytol.* **220**, 1148–1160. (doi:10.1111/nph.15203)
9. Rowan R, Knowlton N. 1995 Intraspecific diversity and ecological zonation in coral–algal symbiosis. *Proc. Natl Acad. Sci. USA* **92**, 2850–2853. (doi:10.1073/pnas.92.7.2850)
10. Iglesias-Prieto R, Beltrán VH, LaJeunesse TC, Reyes-Bonilla H, Thomé PE. 2004 Different algal symbionts explain the vertical distribution of dominant reef corals in the Eastern Pacific. *Proc. R. Soc. Lond. B* **271**, 1757–1763. (doi:10.1098/rspb.2004.2757)
11. Sampayo EM, Ridgway T, Bongaerts P, Hoegh-Guldberg O. 2008 Bleaching susceptibility and mortality of corals are determined by fine-scale differences in symbiont type. *Proc. Natl Acad. Sci. USA* **105**, 10 444–10 449. (doi:10.1073/pnas.0708049105)
12. Bongaerts P, Carmichael M, Hay KB, Tonk L, Frade PR, Hoegh-Guldberg O. 2015 Prevalent endosymbiont zonation shapes the depth distributions of scleractinian coral species. *R. Soc. open sci.* **2**, 140297. (doi:10.1098/rsos.140297)
13. Cox F, Barsoum N, Lilleskov EA, Bidartondo MI. 2010 Nitrogen availability is a primary determinant of conifer mycorrhizas across complex environmental gradients. *Ecol. Lett.* **13**, 1103–1113. (doi:10.1111/j.1461-0248.2010.01494.x)
14. Kjøller R, Nilsson L-O, Hansen K, Schmidt IK, Vesterdal L, Gundersen P. 2012 Dramatic changes in ectomycorrhizal community composition, root tip abundance and mycelial production along a stand-scale nitrogen deposition gradient. *New Phytol.* **194**, 278–286. (doi:10.1111/j.1469-8137.2011.04041.x)

15. Suz LM *et al.* 2014 Environmental drivers of ectomycorrhizal communities in Europe's temperate oak forests. *Mol. Ecol.* **23**, 5628–5644. (doi:10.1111/mec.12947)
16. Fernández-Mendoza F, Domaschke S, García MA, Jordan P, Martín MP, Printzen C. 2011 Population structure of mycobionts and photobionts of the widespread lichen *Cetraria aculeata*. *Mol. Ecol.* **20**, 1208–1232. (doi:10.1111/j.1365-294X.2010.04993.x)
17. Grande FD, Rolshausen G, Divakar PK, Crespo A, Otte J, Schleuning M, Schmitt I. 2018 Environment and host identity structure communities of green algal symbionts in lichens. *New Phytol.* **217**, 277–289. (doi:10.1111/nph.14770)
18. Rolshausen G, Dal Grande F, Sadowska-Deś AD, Otte J, Schmitt I. 2018 Quantifying the climatic niche of symbiont partners in a lichen symbiosis indicates mutualist-mediated niche expansions. *Ecography* **41**, 1380–1392. (doi:10.1111/ecog.03457)
19. Peay KG. 2016 The mutualistic niche: mycorrhizal symbiosis and community dynamics. *Annu. Rev. Ecol. Evol. Syst.* **47**, 143–164. (doi:10.1146/annurev-ecolsys-121415-032100)
20. Batstone RT, Carscadden KA, Afkhami ME, Frederickson ME. 2018 Using niche breadth theory to explain generalization in mutualisms. *Ecology* **99**, 1039–1050. (doi:10.1002/ecy.2188)
21. Thomas CD, Bodsworth EJ, Wilson RJ, Simmons AD, Davies ZG, Musche M, Conradt L. 2001 Ecological and evolutionary processes at expanding range margins. *Nature* **411**, 577–581. (doi:10.1038/35079066)
22. Hampe A, Petit RJ. 2005 Conserving biodiversity under climate change: the rear edge matters. *Ecol. Lett.* **8**, 461–467. (doi:10.1111/j.1461-0248.2005.00739.x)
23. Pearman PB, Guisan A, Broennimann O, Randin CF. 2008 Niche dynamics in space and time. *Trends Ecol. Evol.* **23**, 149–158. (doi:10.1016/j.tree.2007.11.005)
24. Angert AL. 2009 The niche, limits to species' distributions, and spatiotemporal variation in demography across the elevation ranges of two monkeyflowers. *Proc. Natl Acad. Sci. USA* **106**, 19 693–19 698. (doi:10.1073/pnas.0901652106)
25. Lenoir J, Svenning J-C. 2015 Climate-related range shifts: a global multidimensional synthesis and new research directions. *Ecography* **38**, 15–28. (doi:10.1111/ecog.00967)
26. Rumpf SB, Hülber K, Zimmermann NE, Dullinger S. 2019 Elevational rear edges shifted at least as much as leading edges over the last century. *Global Ecol. Biogeogr.* **28**, 533–543. (doi:10.1111/geb.12865)
27. Helmuth B, Kingsolver JG, Carrington E. 2005 Biophysics, physiological ecology, and climate change: does mechanism matter? *Annu. Rev. Physiol.* **67**, 177–201. (doi:10.1146/annurev.physiol.67.040403.105027)
28. Gilman SE, Urban MC, Tewksbury J, Gilchrist GW, Holt RD. 2010 A framework for community interactions under climate change. *Trends Ecol. Evol.* **25**, 325–331. (doi:10.1016/j.tree.2010.03.002)
29. Kokko H, Chaturvedi A, Croll D, Fischer MC, Guillaume F, Karrenberg S, Kerr B, Rolshausen G, Stapley J. 2017 Can evolution supply what ecology demands? *Trends Ecol. Evol.* **32**, 187–197. (doi:10.1016/j.tree.2016.12.005)
30. Kiers ET, Palmer TM, Ives AR, Bruno JF, Bronstein JL. 2010 Mutualisms in a changing world: an evolutionary perspective. *Ecol. Lett.* **13**, 1459–1474. (doi:10.1111/j.1461-0248.2010.01538.x)
31. Lankau RA, Keymer DP. 2016 Ectomycorrhizal fungal richness declines towards the host species' range edge. *Mol. Ecol.* **25**, 3224–3241. (doi:10.1111/mec.13628)
32. Kappen L. 1988 Ecophysiological relationships in different climatic regions. In *Handbook of lichenology* (ed. M Galun), pp. 37–100. Boca Raton, FL: CRC Press.
33. Honegger R. 1991 Functional aspects of the lichen symbiosis. *Annu. Rev. Plant Biol.* **42**, 553–578. (doi:10.1146/annurev.pp.42.060191.003005)
34. Kranner I, Beckett R, Hochman A, Nash TH. 2008 Desiccation-tolerance in lichens: a review. *The Bryologist* **111**, 576–593. (doi:10.1639/0007-2745-111.4.576)
35. Piercey-Normore MD, DePriest PT. 2001 Algal switching among lichen symbioses. *Am. J. Bot.* **88**, 1490–1498. (doi:10.2307/3558457)
36. Piercey-Normore MD. 2006 The lichen-forming ascomycete *Evernia mesomorpha* associates with multiple genotypes of *Trebouxia jamesii*. *New Phytol.* **169**, 331–344. (doi:10.1111/j.1469-8137.2005.01576.x)
37. Yahr R, Vilgalys R, DePriest PT. 2006 Geographic variation in algal partners of *Cladonia subtenuis* (Cladoniaceae) highlights the dynamic nature of a lichen symbiosis. *New Phytol.* **171**, 847–860. (doi:10.1111/j.1469-8137.2006.01792.x)
38. Muggia L, Pérez-Ortega S, Kopun T, Zellnig G, Grube M. 2014 Photobiont selectivity leads to ecological tolerance and evolutionary divergence in a polymorphic complex of lichenized fungi. *Ann. Bot.* **114**, 463–475. (doi:10.1093/aob/mcu146)
39. Vančurová L, Muggia L, Peksa O, Řídká T, Škaloud P. 2018 The complexity of symbiotic interactions influences the ecological amplitude of the host: a case study in *Stereocaulon* (lichenized Ascomycota). *Mol. Ecol.* **27**, 3016–3033. (doi:10.1111/mec.14764)
40. Arendt J, Reznick D. 2008 Convergence and parallelism reconsidered: what have we learned about the genetics of adaptation? *Trends in Ecol. Evol.* **23**, 26–32. (doi:10.1016/j.tree.2007.09.011)
41. Langerhans RB, DeWitt TJ. 2004 Shared and unique features of evolutionary diversification. *Am. Nat.* **164**, 335–349. (doi:10.1086/422857)
42. Oke KB, Rolshausen G, LeBlond C, Hendry AP. 2017 How parallel is parallel evolution? A comparative analysis in Fishes. *Am. Nat.* **190**, 1–16. (doi:10.1086/691989)
43. Cubero OF, Crespo A. 2002 Isolation of nucleic acids from lichens. In *Protocols in lichenology* (eds IC Kranner, RP Beckett, AK Varma), pp. 381–391. Berlin, Germany: Springer.
44. Kroken S, Taylor JW. 2000 Phylogenetic species, reproductive mode, and specificity of the green alga *Trebouxia* forming lichens with the fungal genus *Letharia*. *The Bryologist* **103**, 645–660. (doi:10.1639/0007-2745(2000)103[0645:PSRMAS]2.0.CO;2)
45. Sadowska-Deś AD, Bálint M, Otte J, Schmitt I. 2013 Assessing intraspecific diversity in a lichen-forming fungus and its green algal symbiont: evaluation of eight molecular markers. *Fungal Ecol.* **6**, 141–151. (doi:10.1016/j.funeco.2012.12.001)
46. Sadowska-Deś AD, Dal Grande F, Lumbsch HT, Beck A, Otte J, Hur J-S, Kim JA, Schmitt I. 2014 Integrating coalescent and phylogenetic approaches to delimit species in the lichen photobiont Trebouxia. *Mol. Phyl. Evol.* **76**, 202–210. (doi:10.1016/j.ympev.2014.03.020)
47. Paul F, Otte J, Schmitt I, Dal Grande F. 2018 Comparing Sanger sequencing and high-throughput metabarcoding for inferring photobiont diversity in lichens. *Sci. Rep.* **8**, 8624. (doi:10.1038/s41598-018-26947-8)
48. Leavitt SD, Kraichak E, Nelsen MP, Altermann S, Divakar PK, Alors D, Esslinger TL, Crespo A, Lumbsch T. 2015 Fungal specificity and selectivity for algae play a major role in determining lichen partnerships across diverse ecogeographic regions in the lichen-forming family Parmeliaceae (Ascomycota). *Mol. Ecol.* **24**, 3779–3797. (doi:10.1111/mec.13271)
49. Stamatakis A. 2014 RAxML version 8: a tool for phylogenetic analysis and post-analysis of large phylogenies. *Bioinformatics* **30**, 1312–1313. (doi:10.1093/bioinformatics/btu033)
50. Hijmans RJ, Cameron SE, Parra JL, Jones PG, Jarvis A. 2005 Very high resolution interpolated climate surfaces for global land areas. *Int. J. Climatol.* **25**, 1965–1978. (doi:10.1002/joc.1276)
51. Wood SN. 2000 Modelling and smoothing parameter estimation with multiple quadratic penalties. *J. R. Statist. Soc. B* **62**, 413–428. (doi:10.1111/1467-9868.00240)
52. Wood SN. 2017 *Generalized additive models: an introduction with R*. Boca Raton, FL: Chapman and Hall/CRC.
53. R Core Team. 2018 *R: a language and environment for statistical computing*. Vienna, Austria: R Foundation for Statistical Computing. See https://www.r-project.org.
54. Oksanen J, Blanchet FG, Kindt R, Legendre P, O'hara RB, Simpson GL, Solymos P, Stevens MHH, Wagner H. 2010 vegan: community ecology package (version 1.17-4). See https://cran.r-project.org.
55. Baselga A, Orme CDL. 2012 betapart: an R package for the study of beta diversity. *Methods Ecol. Evol.* **3**, 808–812. (doi:10.1111/j.2041-210X.2012.00224.x)
56. Wilson MV, Shmida A. 1984 Measuring beta diversity with presence-absence data. *J. Ecol.* **72**, 1055–1064. (doi:10.2307/2259551)
57. Williams PH. 1996 Mapping variations in the strength and breadth of biogeographic transition zones using species turnover. *Proc. R. Soc. Lond. B* **263**, 579–588. (doi:10.1098/rspb.1996.0087)
58. Baselga A. 2012 The relationship between species replacement, dissimilarity derived from nestedness, and nestedness: species replacement and nestedness. *Glob. Ecol. Biogeogr.* **21**, 1223–1232. (doi:10.1111/j.1466-8238.2011.00756.x)

59. Schindler DE, Armstrong JB, Reed TE. 2015 The portfolio concept in ecology and evolution. *Front. Ecol. Env.* **13**, 257–263. (doi:10.1890/140275)
60. Werth S, Sork VL. 2014 Ecological specialization in *Trebouxia* (Trebouxiophyceae) photobionts of *Ramalina menziesii* (Ramalinaceae) across six range-covering ecoregions of western North America. *Am. J. Bot.* **101**, 1127–1140. (doi:10.3732/ajb.1400025)
61. Beck A, Friedl T, Rambold G. 1998 Selectivity of photobiont choice in a defined lichen community: inferences from cultural and molecular studies. *New Phytol.* **139**, 709–720. (doi:10.1046/j.1469-8137.1998.00231.x)
62. Rambold G, Friedl T, Beck A. 1998 Photobionts in lichens: possible indicators of phylogenetic relationships? *The Bryologist* **101**, 392–397. (doi:10.1639/0007-2745(1998)101[392:PILPIO]2.0.CO;2)
63. Doering M, Piercey-Normore MD. 2009 Genetically divergent algae shape an epiphytic lichen community on Jack Pine in Manitoba. *The Lichenologist* **41**, 69–80. (doi:10.1017/S0024282909008111)
64. Metzger MJ, Bunce RGH, Jongman RHG, Sayre R, Trabucco A, Zomer R. 2013 A high-resolution bioclimate map of the world: a unifying framework for global biodiversity research and monitoring: high-resolution bioclimate map of the world. *Glob. Ecol. Biogeogr.* **22**, 630–638. (doi:10.1111/geb.12022)
65. Sonesson M. 1986 Photosynthesis in lichen populations from different altitudes in Swedish lapland. *Polar Biol.* **5**, 113–124. (doi:10.1007/BF00443383)
66. Schipperges B, Kappen L, Sonesson M. 1995 Intraspecific variations of morphology and physiology of temperate to arctic populations of *Cetraria nivalis*. *Lichenologist* **27**, 517–529. (doi:10.1016/S0024-2829(95)80011-5)
67. Gaio-Oliveira G, Dahlman L, Máguas C, Palmqvist K. 2004 Growth in relation to microclimatic conditions and physiological characteristics of four *Lobaria pulmonaria* populations in two contrasting habitats. *Ecography* **27**, 13–28. (doi:10.1111/j.0906-7590.2004.03577.x)
68. Sonesson M, Sveinbjörnsson B, Tehler A, Carlsson BÅ. 2007 A comparison of the physiology, anatomy and ribosomal DNA in alpine and subalpine populations of the lichen *Nephroma arcticum*—the effects of an eight-year transplant experiment. *Bryologist* **110**, 244–253. (doi:10.1639/0007-2745(2007)110[244:ACOTPA]2.0.CO;2)
69. Casano LM, del Campo EM, García-Breijo FJ, Reig-Armiñana J, Gasulla F, del Hoyo A, Guéra A, Barreno E. 2011 Two Trebouxia algae with different physiological performances are ever-present in lichen thalli of *Ramalina farinacea:* coexistence versus competition? *Env. Microbiol.* **13**, 806–818. (doi:10.1111/j.1462-2920.2010.02386.x)
70. Determeyer-Wiedmann N, Sadowsky A, Convey P, Ott S. 2019 Physiological life history strategies of photobionts of lichen species from Antarctic and moderate European habitats in response to stressful conditions. *Pol. Biol.* **42**, 395–405. (doi:10.1007/s00300-018-2430-2)
71. Domaschke S, Vivas M, Sancho LG, Printzen C. 2013 Ecophysiology and genetic structure of polar versus temperate populations of the lichen *Cetraria aculeata*. *Oecologia* **173**, 699–709. (doi:10.1007/s00442-013-2670-3)
72. Svensson M, Caruso A, Yahr R, Ellis C, Thor G, Snäll T. 2016 Combined observational and experimental data provide limited support for facilitation in lichens. *Oikos* **125**, 278–283. (doi:10.1111/oik.02279)
73. Kraft NJB, Adler PB, Godoy O, James EC, Fuller S, Levine JM. 2015 Community assembly, coexistence and the environmental filtering metaphor. *Funct. Ecol.* **29**, 592–599. (doi:10.1111/1365-2435.12345)
74. Cadotte MW, Tucker CM. 2017 Should environmental filtering be abandoned? *Trends Ecol. Evol.* **32**, 429–437. (doi:10.1016/j.tree.2017.03.004)
75. Rolshausen G, Hallman U, Grande FD, Otte J, Knudsen K, Schmitt I. 2020 Data from: Expanding the mutualistic niche: parallel symbiont turnover along climatic gradients. Dryad Digital Repository. (doi:10.5061/dryad.qv9s4mw9s)